Am J Cancer Res 2023;13(8):3547-3558
www.ajcr.us /ISSN:2156-6976/ajcr0151623

Original Article

ATRX loss suppresses the type I interferon response in sarcoma cells through chromatin remodeling

Xinrui Wang*, Zige Jin*, Shanshan Tang, Xiyu Huang, Shanshan Wang, Xiaohe Ren, Mafei Xu

*Department of Cell Biology, School of Life Sciences, Anhui Medical University, Hefei 230032, Anhui, China. *Equal contributors.*

Received June 7, 2023; Accepted July 30, 2023; Epub August 15, 2023; Published August 30, 2023

Abstract: Sarcomas constitute a heterogeneous group of mesenchymal cancers and are particularly common in children and adolescents, leading to significant lethality. Therefore, it is necessary to understand the underlying mechanisms by which genetic alterations promote sarcoma progression. Here, we demonstrate that loss-of-function of *ATRX*, a member of the SWI/SNF DNA-remodeling family, represses the interferon (IFN)-β response by inducing chromatin remodeling in sarcoma cells. We show that *ATRX* mutations are associated with worse prognosis and attenuate IFN-α/β response in patients with specific types of sarcomas. Using poly(I:C) as a stimulation model, we show that natural ATRX mutation or ATRX depletion via CRISPR/Cas9 or siRNA significantly suppresses the expression of IFNB1 and other cytokines in sarcoma cells. Moreover, RNA-seq data reveal that ATRX ablation globally influences the expression pattern of poly(I:C)-stimulated genes (PSGs). Through ATAC-seq, we show that ATRX loss enhance chromatin accessibility generally, which consistent with the heterochromatin modulating function of ATRX. However, a set of PSGs display a decrease of chromatin accessibility after ATRX depletion, indicating that ATRX promote the transcription of these genes through chromatin remodeling. Thus, we highlight that *ATRX* mutation plays critical roles in blocking Type I IFN signaling in sarcoma cells and point out the clinical importance of this effect on sarcoma treatment.

Keywords: ATRX, sarcoma, type I interferon, antitumor immunity, chromatin remodeling

Introduction

Sarcomas are rare malignancies, collectively accounting for only 1% of adult and 15% of pediatric cancers [1, 2]. There are at least 100 types of sarcomas, as identified on the basis of distinct morphological and genetic changes, such as osteosarcoma, angiosarcoma, and Ewing sarcoma. To date, the standard treatments for sarcomas include surgery, chemotherapy and radiotherapy, but the outcomes are unsatisfactory. Globally, the 5-year relative survival rate of sarcoma patients is approximately 50%, and it is less than 20% for patients with distant metastasis [3, 4]. Recently, immunotherapy has become an important clinical strategy for certain types of advanced cancers, such as melanoma, non-small-cell lung cancer (NSCLC) and bladder cancer [5-8]. However, clinical trials have revealed that sarcoma cells do not respond adequately to immunotherapies, which include immune checkpoint inhibitors, adoptive cell therapies, and cancer vaccines [3], mainly due to the diminished effects of the immune microenvironment in the context of sarcoma [9, 10]. Therefore, investigating the underlying mechanisms by which sarcoma cells modulate the antitumor immune response is crucial.

Type I interferon (IFN) signaling can be stimulated by danger-associated molecular patterns (DAMPs) in the tumor microenvironment (TME), then activate the innate immune response against tumors through the action of cytotoxic T lymphocytes (CTLs), natural killer (NK) cells, dendritic cells (DCs) and cancer cells themselves [11, 12]. For instance, cytosolic RNA and DNA activate the retinoic acid-inducible gene I (RIG-I) and Cyclic guanosine monophosphate-adenosine monophosphate adenosine synthetase (cGAS) pathways, respectively, leading to the transcription of Type I IFNs and hundreds of IFN-stimulated genes (ISGs) [12, 13]. Nevertheless, these pathways are commonly suppressed in cancer cells through the downregulation of

DAMP receptors and activation of immune checkpoint signaling [3, 9, 13]. A recent study revealed that in sarcoma cells, RIG-I-mediated Type I IFN signaling was suppressed by circRNAs, leading to the establishment of a protumorigenic TME and increased tumor growth [14]. Due to the heterogeneity of sarcomas, it is still unclear how type I IFN signaling is modulated in different types of sarcoma cells.

ATRX is a member of the switch/sucrose nonfermentable (SWI/SNF) protein family, and serves as a DNA remodeler for heterochromatin formation and transcription regulation [15]. *ATRX* mutations cause alpha thalassemia/mental retardation X-linked (ATRX) syndrome and is associated with alternative lengthening of telomeres (ALT) in cancer cells [15, 16]. Notably, ATRX mutation is frequent in sarcoma, with frameshift and nonsense mutations as the most prevalent variations, suggesting that ATRX loss might drive sarcoma progression [17, 18]. A recent study reported that loss of *ATRX* promoted the aggressiveness of osteosarcoma through upregulating NF-κB signaling and integrin binding [19]. Moreover, *ATRX* deletion impaired cGAS/STING signaling and sensitized sarcoma to radiation and oncolytic herpesvirus [20]. In addition, in ALT cancer cells, telomeric DNA accumulated in the cytoplasm due to telomere instability, while the induction of the innate immune response was suppressed by ATRX depletion [21]. This evidence raises interesting questions relating to whether and how ATRX mutations alter type I IFN-mediated antitumor immune responses in sarcomas.

In the present study, we analyzed public datasets and observed that *ATRX* mutations were negatively correlated with prognosis and type I interferon response in patients with specific types of sarcomas. Through RNA-seq and ATAC-seq, we further revealed that ATRX loss reduced the chromatin accessibility and transcript of IFN-β and a set of ISGs in sarcoma cells. Thus, our findings highlight that ATRX mutations play critical roles in suppressing Type I IFN response in sarcoma.

Materials and methods

Cell culture

HOS, MG63, U2OS, Saos-2 and 293T cells were purchased from Procell Life Science & Technology Co., Ltd. (CL-0360, CL0157, CL-0236, CL-0202, CL-0469). All cells were cultured with 5% CO_2 at 37°C in an incubator. HOS and MG63 cells were cultured in MEM supplemented with NEAA and 10% FBS. U2OS cells were cultured in McCoy's 5A medium supplemented with 10% FBS. Saos-2 cells were cultured in McCoy's 5-A medium supplemented with 15% FBS. 293T cells were cultured in DMEM supplemented with 10% FBS. Cell lines were authenticated by STR DNA profiling analysis and tested to confirm the lack of mycoplasma contamination.

Plasmid construction

LentiCas9-Blast (Plasmid #52962) and LentiGuide-puro (Plasmid #52962) were purchased from Addgene; pCMVdeltaR8.9 and pLP-VSVg were stocked in our laboratory. sgRNA expression plasmids targeting the human ATRX gene were designed by CRISPick. Oligos were synthesized by Tsingke Biotechnology Co., Ltd. The sgRNA sequences were: sghATRX-238-F: CACCGCAGGATCGTCACGATCAAAG; sghATRX-238-R: AAACCTTTGATCGTGACGATCCTGC; sghATRX-672-F: CACCGCAATGTAGGTGGTGTGCGGA; sghATRX-672-R: AAACTCCGCACACCACCTACATTGC. Paired oligos were annealed and then inserted into BsmB I site of the LentiGuide-puro vector.

Lentivirus packaging and infection

293T cells were transfected with lentivirus-expressing plasmid, pCMVdeltaR8.9 and pLP-VSVg by polyethylenimine (PEI). The infectious supernatants were harvested 72 hours after transfection, filtered through a 0.45-μM filter, and stored at -80°C. To infect HOS cells, supernatants were mixed with polybrene at a final concentration of 5 μg/mL, and with HOS medium at a 1:1 ratio, then added to HOS cells grown to 50%-60% density. After 48 hours, the positive cells were selected after treatment with a final concentration of 1 μg/ml puromycin (Meilunbio; MA0318) or 10 μg/ml blasticidin (Meilunbio; MB2506-1).

Western blotting

Cells were lysed in RIPA lysis buffer (Beyotime, P0013B), incubated at 4°C for 15 minutes, and then clarified by centrifugation at 14000 × g and 4°C for 15 minutes. The clarified lysates were mixed with SDS-PAGE Sample Loading Buffer (Beyotime, P0015L) and boiled for 10 min. Equal amounts of total protein were resolved on 8% SDS-PAGE gels (Beyotime, SDS-PAGE Gel Preparation Kit, P0012A) in 1X run-

ning buffer (25 mM Tris, 0.25 M glycine, 0.1% SDS) and then transferred to NC membranes (Merck Millipore; HATF00010) for immunoblotting. The antibodies used for western blotting were anti-ATRX, Abcam, ab97508; anti-alpha tubulin, Proteintech, 11224-1-AP; and HRP-labeled goat anti-rabbit IgG (H+L), ZSGB-BIO, ZB-2301.

Transfection with dsDNA or poly(I:C)

Cells were cultured in 12-well plates and transfected with 1 μg poly(I:C) (Invivogen tlrl-pic) or 1 μg dsDNA (Tsingke Biotechnology Co. Ltd.) via the standard protocol of Lipofectamine 2000 (Invitrogen™; 11668027). Cells were harvested at different time points for RNA extraction and real-time qPCR analysis. RNA was extracted using a SPARKeasy Cell RNA Rapid Extraction Kit (SparkJade; AC0205-B). cDNA was obtained by reverse transcription using MonScript™ RTIII All-in-One Mix with dsDNase kit (Monad; MR05101). Real-time qPCR was performed on a Roche Light Cycler 96 using ChamQ Universal SYBR qPCR Master Mix (Vazyme; Q711). The following primers were synthesized by Tsingke Biotechnology Co., Ltd.: IFNB1-F: ATGACCAACAAGTGTCTCCTCC; IFNB1-R: GGAATCCAAGCAAGTTGTAGCTC; CXCL10-F: GTGGCATTCAAGGAGTACCTC; CXCL10-R: TGATGGCCTTCGATTCTGGATT; GAPDH-F: CATGAGAAGTATGACAACAGCCT; GAPDH-R: AGTCCTTCCACGATACCAAAGT; IL6-F: ACTCACCTCTTCAGAACGAATTG; IL6-R: CCATCTTTGGAAGGTTCAGGTTG; MX1-F: GTTTCCGAAGTGGACATCGCA; MX1-R: CTGCACAGGTTGTTCTCAGC; MX2-F: CAGAGGCAGCGGAATCGTAA; MX2-R: TGAAGCTCTAGCTCGGTGTTC.

RNA-seq and analysis

Total RNA was extracted with a SPARKeasy Cell RNA Rapid Extraction Kit (SparkJade; AC0205-B) and subjected to RNA-seq on a MGISEQ-2000 platform in PE150 mode by BGI Tech Solutions Co., Ltd. Transcript reads were quantified by salmon with default settings and mapped to the reference genome (hg19) using the Bowtie tool. Differential expression analysis was performed with the R package DESeq2 at an adjusted *p* value cutoff <0.05. Gene set enrichment analysis was performed with GSEA 4.1.0; heatmaps and volcano plots were generated with the R packages pheatmap and enhanced volcano. GO enrichment analysis was performed with clusterProfiler.

ATAC-seq and analysis

Cells were lysed in NE buffer (10 mM Tris-HCl, pH 7.4; 10 mM NaCl; 3 mM $MgCl_2$; and 0.1% IGEPAL CA-630) and subjected to DNA tagmentation using TruePrep DNA Library Prep Kit V2 for Illumina kit (Vazyme TD501). After tagmentation, the DNA was purified by VAHTS DNA Clean Beads (Vazyme N411-01). Libraries were amplified by PCR, and indexes were added by TruePrep™ Index Kit V2 for Illumina® (Vazyme TD202), subjected to sequencing on a NovaSeq system by Berry Genomics. For analysis, reads were aligned to the UCSC hg19 reference genome, and duplications were removed by sambamba. Then, peaks were called by the MACS3 command callpeak. Differential analysis was performed via the MACS3 command bdgdiff. Visualization was performed with deeptools and IGV. Annotation was performed via ChIPseeker. GO enrichment analysis was performed with Cistrome-GO. Motif analysis was performed with HOMER software.

Clinical data analysis

Patient survival and ATRX alternation data were obtained from TCGA Pan Cancer Atlas and MSK Sarcoma datasets using cBioPortal. For GSEA, TCGA pancancer atlas sarcoma patient gene expression data were classified into two groups according to ATRX mutation status, and GSEA was then performed by using the GSEA 4.1.0 and MSigDB v7.4 databases.

Statistical analysis

GraphPad Prism 9.0 was used for statistical analysis. Specifically, log-rank tests were performed via GraphPad Prism 9.0. For all comparisons among three groups, two-way ANOVAs followed by multiple comparisons were performed; *: *P* value <0.05; **: *P* value <0.01; and ***: *P* value <0.001.

Data and code availability

The raw sequence data reported in this paper have been deposited in the Genome Sequence Archive [22] in National Genomics Data Center, China National Center [23] for Bioinformation/Beijing Institute of Genomics, Chinese Academy of Sciences (GSA-Human: HRA005116) that are publicly accessible at https://ngdc.cncb.ac.cn/gsa-human.

Results

ATRX mutation showed clinical relevance to prognosis and IFN-β signaling in subtypes of sarcomas

To understand the clinical importance of *ATRX* mutation in different types of sarcomas, we analyzed the MSK and TCGA pancancer atlas datasets in cBioPortal. As shown in **Figure 1A**, *ATRX* gene was more frequently altered in samples of uterine leiomyosarcoma, undifferentiated pleomorphic sarcoma, leiomyosarcoma, angiosarcoma, dedifferentiated liposarcoma and osteosarcoma and less frequently altered in samples of Ewing sarcoma and gastrointestinal sarcoma. Interestingly, *ATRX* mutation was associated with worse overall survival times in patients with leiomyosarcoma and osteosarcoma (**Figure 1B-D**) but not in patients with other types of sarcomas (**Figure 1E** and **1F**). These data suggest that the effects of ATRX loss are mediated in a cancer type-dependent manner.

Furthermore, we analyzed the RNA-seq data obtained from the TCGA dataset by GSEA and revealed the top hallmark pathways associated with ATRX mutation. As shown in **Figure 1G**, ATRX loss upregulated cell proliferation pathways, such as pathways associated with E2F1 targets, the mitotic spindle, and G2/M checkpoints, as well as stress-induced pathways, including the TNF-A, apoptosis, ROS and inflammatory response pathways. On the other hand, pathways associated with estrogen and androgen response genes and KRAS downregulated genes were suppressed after functional ATRX loss. Notably, the expression of INF-α response genes was also negatively correlated with ATRX mutants, NES = -0.93 (**Figure 1H**). Although the difference was not significant, this result indicates that ATRX loss might reduce type-I interferon signaling in sarcoma cells.

The expression of IFNB1 and ISGs was suppressed in sarcoma cells with ATRX mutations

In the tumor microenvironment, type I interferon can be induced by cytosolic DNA and RNA through the cGAS/STING and RIG-1/MAVS pathway, respectively [12, 13, 24]. Therefore, we evaluated the response of sarcoma cells with different status of ATRX gene after exposure to double-stranded DNA (dsDNA) or poly(I:C), a synthetic analog of double-stranded RNA. As shown in **Figure 2A**, ATRX was expressed in HOS and MG63 cells but was undetectable in ATRX-mutated U2OS and Saos-2 cells. To our surprise, none of these cell lines responded to dsDNA stimulation, as measured by IFNB1 and CXCL10 expression (**Figure 2B** and **2C**), suggesting that the cGAS/STING pathway is typically blocked in sarcoma cells. In contrast, poly(I:C) induced IFNB1 and CXCL10 expression in all the cells, but the expression levels in HOS and MG63 cells were markedly higher than those in U2OS and Saos-2 cells (**Figure 2B** and **2C**). These results were consistent with the GSEA results obtained with in patient samples, indicating that ATRX mutation is associated with the suppression of type-I interferon signaling in sarcoma.

Depletion of ATRX inhibited IFNB1 and ISG expression after poly(I:C) stimulation

To evaluate whether ATRX ablation leads to the suppression of IFNB1 or ISG expression, we designed two sgRNAs targeting *ATRX* and generated *ATRX*-knockout cell lines via CRISPR/Cas9 (**Figure 3A** and **3B**), then evaluated the expression levels of IFNB1 and ISG after poly(I:C) stimulation. As shown in **Figure 3C**, ATRX knockout significantly decreased poly(I:C)-induced expression of IFNB1 and other ISGs. Since the generation of stable cells by lentiviruses takes a long time, we designed two siRNAs to knockdown ATRX, which was accomplished in 3 days (**Figure 3D**), and then measured whether depletion of ATRX in short-term also affect the expression of IFNB1 and ISGs. In both MG63 (**Figure 3E**) and HOS cells (**Figure 3F**), knockdown of ATRX significantly decreased poly(I:C)-induced IFNB1 and ISG expression. These results indicate that ATRX directly regulated IFNB1 and ISG expression after poly(I:C) stimulation, confirming critical roles for ATRX loss in the suppression of the type I interferon response.

ATRX ablation globally modulated the transcriptome of poly(I:C) induced genes

In response to DAMPs stimulation, hundreds of genes associated with innate immunity are activated. To obtain a comprehensive view of the genes regulated by ATRX, we performed RNA-seq to compare the transcriptomes of HOS cells under different siRNA and poly(I:C) treatment conditions. As shown in **Figure 4A**, using $|Log_2FC| \geq 0.583$ as the cutoff, only 7 genes were upregulated, and 3 genes were downregulated after ATRX knockdown under

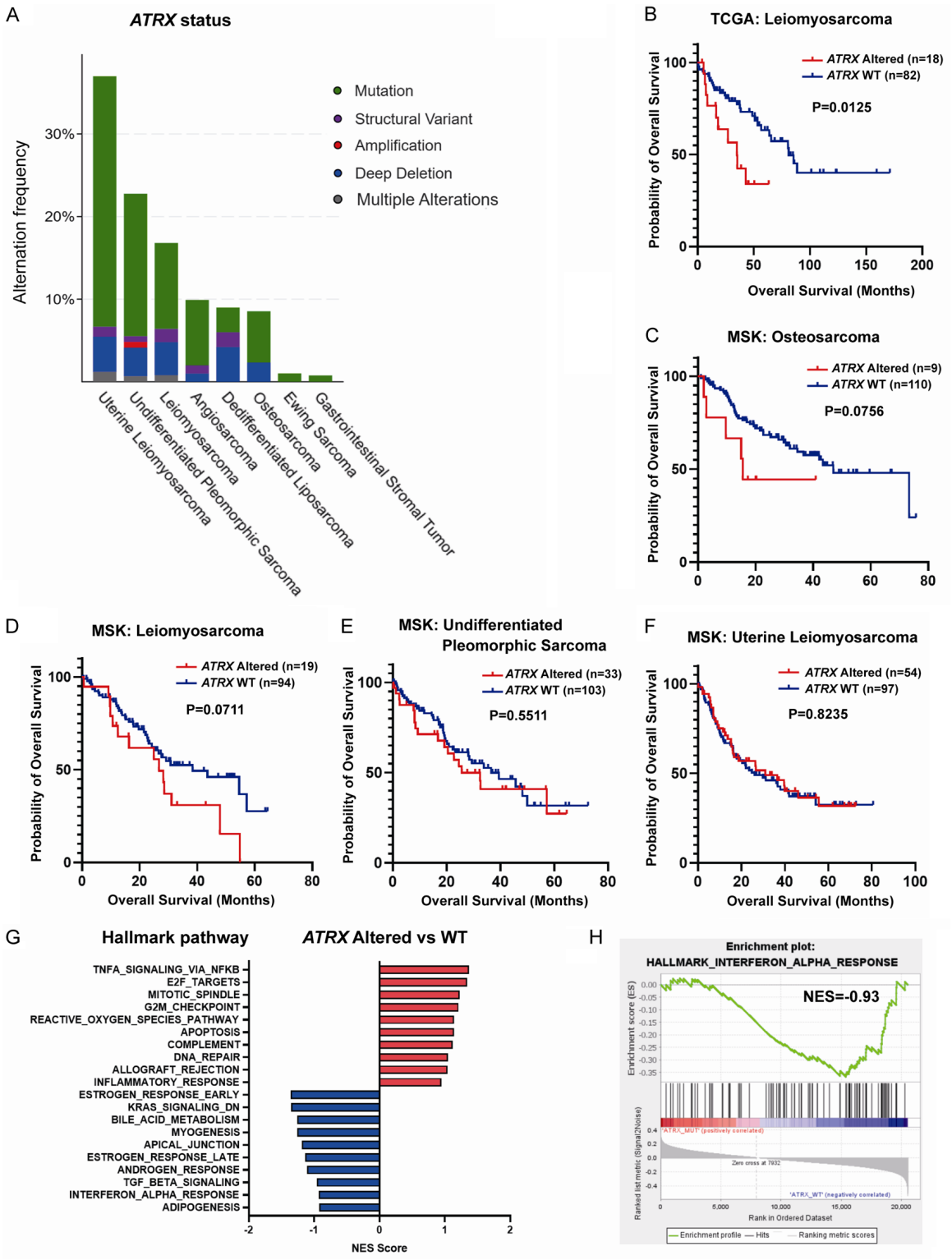

Figure 1. The clinical significance of *ATRX* mutations in sarcoma. A. *ATRX* mutation frequency in different types of sarcomas. The data from MSK and the types of genetic mutations are shown on the right. B-F. Overall survival curves for different types of sarcoma patients with or without *ATRX* mutations. G. GSEA revealed the top hallmark pathways associated with ATRX mutations. H. Gene set enrichment plots showing that the differentially expressed genes belonging to the IFN-α response pathway were negatively correlated with ATRX mutants, NES = -0.93.

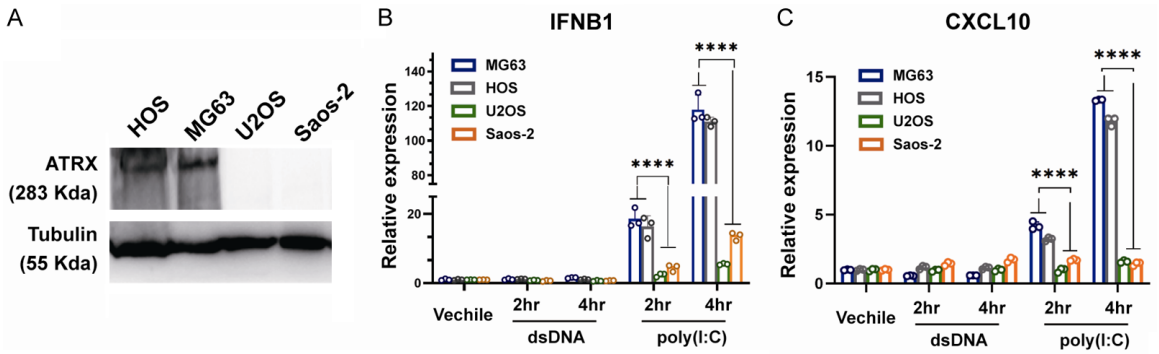

Figure 2. Sarcoma cells with *ATRX* mutations showed reduced poly(I:C)-stimulated gene expression. A. Western blot analysis of ATRX expression in different sarcoma cell lines. ATRX was clearly expressed in HOS and MG63 cells but was undetectable in U2OS and Saos-2 cells. Tubulin was used as the loading control. B, C. Real-time PCR was performed to measure the expression of IFNB1 and CXCL10 in different cells after dsDNA or poly(I:C) treatment. Vehicle represents the control group. The expression level was normalized to that of GAPDH, ****: *P* Value <0.0001.

unstimulated conditions. In contrast, after poly(I:C) stimulation, ATRX depletion resulted in the upregulation of 190 genes and the downregulation of 86 genes (**Figure 4B**). These results suggest that ATRX functions mainly as a transcription regulator not a transcription initiator.

Interestingly, GO analysis revealed that the genes downregulated after siATRX treatment were enriched in type I IFN signaling and antiviral response (**Figure 4C**), consistent with the critical roles of ATRX in the innate immune response. Moreover, using $|Log_2FC| \geq 4$ as the cutoff, we identified 80 upregulated genes and 10 downregulated genes after poly(I:C) treatment in siNC cells (**Figure 4D**), and these genes were defined as poly(I:C)-stimulated genes (PSGs). Most of these PSGs were associated with the innate immune response; specifically, the expression of IFNB1/L2, MX1/2, CXCL8/9/10/11 and IL6 was suppressed by ATRX knockdown following a similar pattern (**Figure 4E**). Thus, our results highlight ATRX ablation globally modulates the transcription of poly(I:C)-induced genes.

ATRX loss changes the chromatin accessibility of PSGs

Next, we assessed the mechanisms by which ATRX regulates PSG expression. Depletion of ATRX changed the expression of a few genes under unstimulated conditions, and none of these genes were involved in cytosolic RNA sensing, suggesting that ATRX may not influence upstream signaling. Therefore, we hypothesized that ATRX may directly modulate the chromatin accessibility of PSGs. To test this hypothesis, we performed ATAC-seq with HOS cells transfected with siRNAs and stimulated with poly(I:C). As shown in **Figure 5A**, depletion of ATRX led to an increase of ATAC-seq signals in 2949 peaks, and a decrease in 282 peaks, these peaks were identified as siATRX gain and loss peaks, respectively. Notably, the siATRX gain peaks were enriched in promoter regions, and siATRX lost peaks were enriched in intron and distal intergenic regions. GO enrichment analysis revealed that siATRX gain peaks were significantly related to genes in chromosome programming, mitosis and transcription regulation (**Figure 5B** and **5C**). These results suggest that ATRX functions mainly as a transcription suppressor. However, the gene bodies of a subset of PSGs, including *IL6*, *MX1/2*, and *CCL2*, displayed less chromatin accessibility after ATRX depletion (**Figure 5D**). Notably, the chromatin accessibility of two enhancer-harboring regions in *IFNB1* was reduced after ATRX knockdown, but the accessibility of gene bodies was unchanged. Moreover, we analyzed the binding motifs of siATRX loss peaks, and KLF4- and NFKB-associated motifs were enriched (**Figure 5E**), these two transcription factors had been reported to regulate type I IFN signaling [25, 26]. Taken together, our study reveals that ATRX loss changed the chromatin accessibility of a subset of PSGs, thereby suppressed the type I IFN axis in sarcoma.

Discussion

In the past decade, a deeper understanding of antitumor immunity has led to great improvements in cancer treatment. Sarcoma is a type

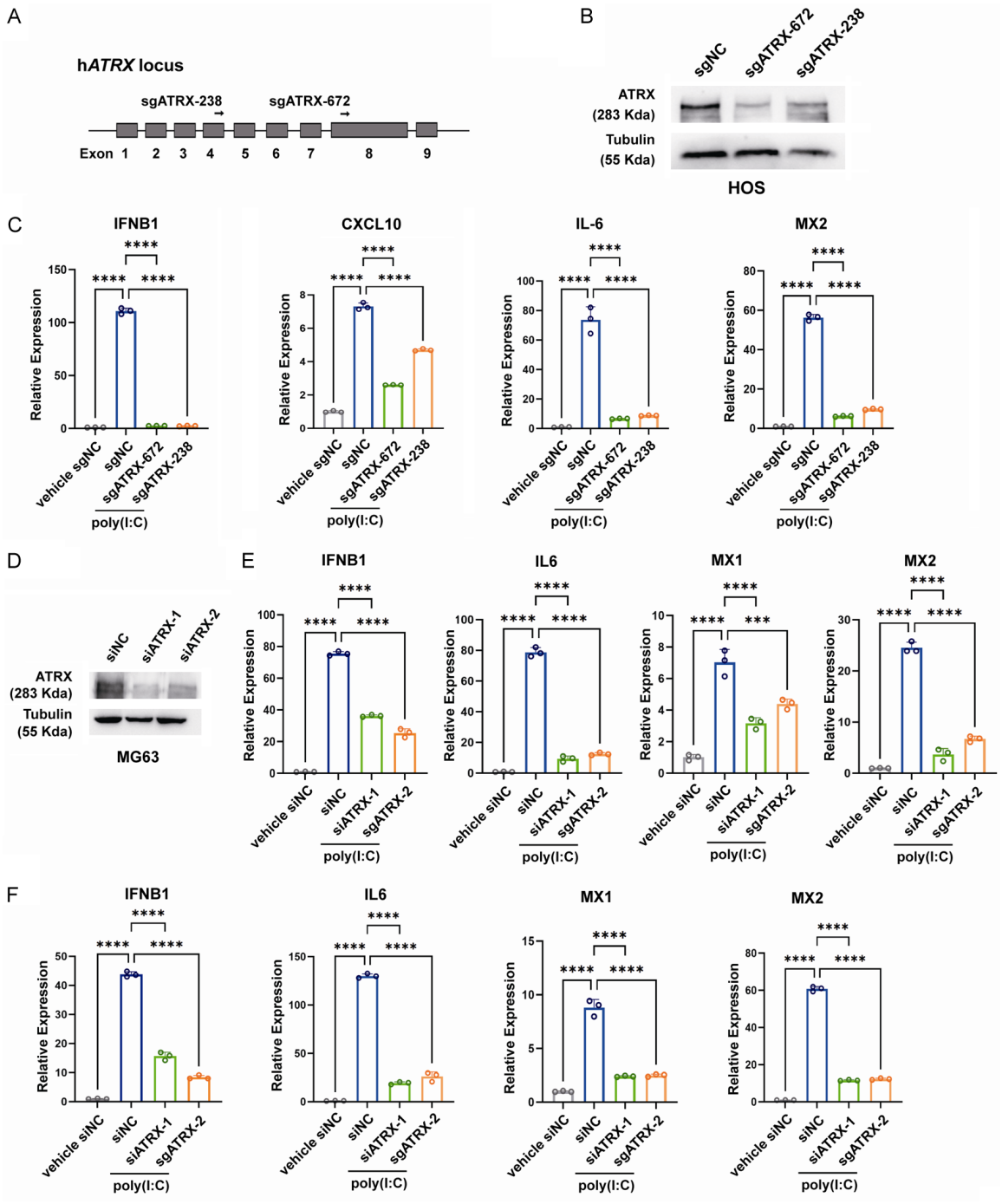

Figure 3. Depletion of ATRX inhibited poly(I:C)-induced expression of immune response genes. (A) Diagram showing the sgRNAs targeting *ATRX*. The numbers indicate Cas9 cut sites from the perspective of the start codon. (B) Western blots showing the knockout efficiency of *ATRX* in HOS cells after Cas9 treatment and the transfection of different sgRNAs. Tubulin was used as the loading control. (C) Real-time PCR was performed to measure the expression of IFNB1, CXCL10, IL6 and MX2 in different cells after poly(I:C) treatment. Vehicle represents the control group. (D) Western blot analysis of the knockdown efficiency of *ATRX* in MG63 cells after transfection with different siRNAs. Tubulin was used as the loading control. (E and F) Real-time PCR was performed to measure the expression of IFNB1, IL6, MX1 and MX2 after poly(I:C) treatment in MG63 (E) or HOS (F) cells transfected with different siRNAs as described. Vehicle represents the control group. The expression level was normalized to that of GAPDH, ****: *P* Value <0.0001.

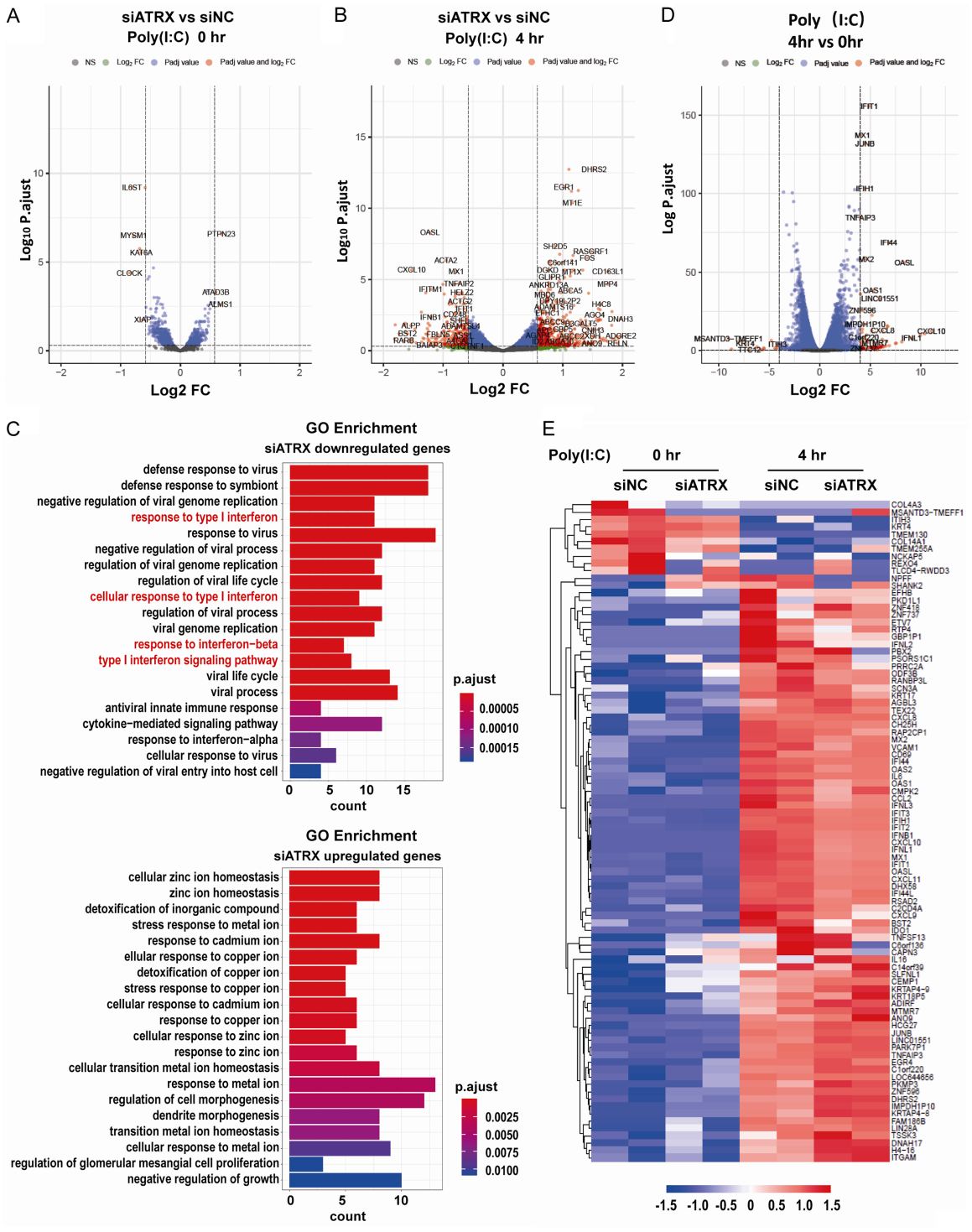

Figure 4. ATRX globally modulated PSG transcription. (A and B) Volcano plot showing differences in the transcript levels of the HOS cells after poly(I:C) stimulation for 0 hr (A) or 4 hr (B). (C) GO enrichment analysis of upregulated and downregulated genes in cells treated with siATRX and stimulated with poly(I:C). (D) Volcano plot showing the differences in siNC HOS transcript levels after poly(I:C) stimulation for the indicated times. (E) Heatmap clusters displaying PSG expression patterns in HOS cells under the indicated siRNA and poly(I:C) treatment conditions.

of "cold" tumor, and its immunosuppressive microenvironment might be one of the major reasons for poor prognosis of patients with sarcomas [3, 4, 9]. Therefore, it is important to understand the detailed mechanisms underlying the "cold" of sarcoma, and develop targeted

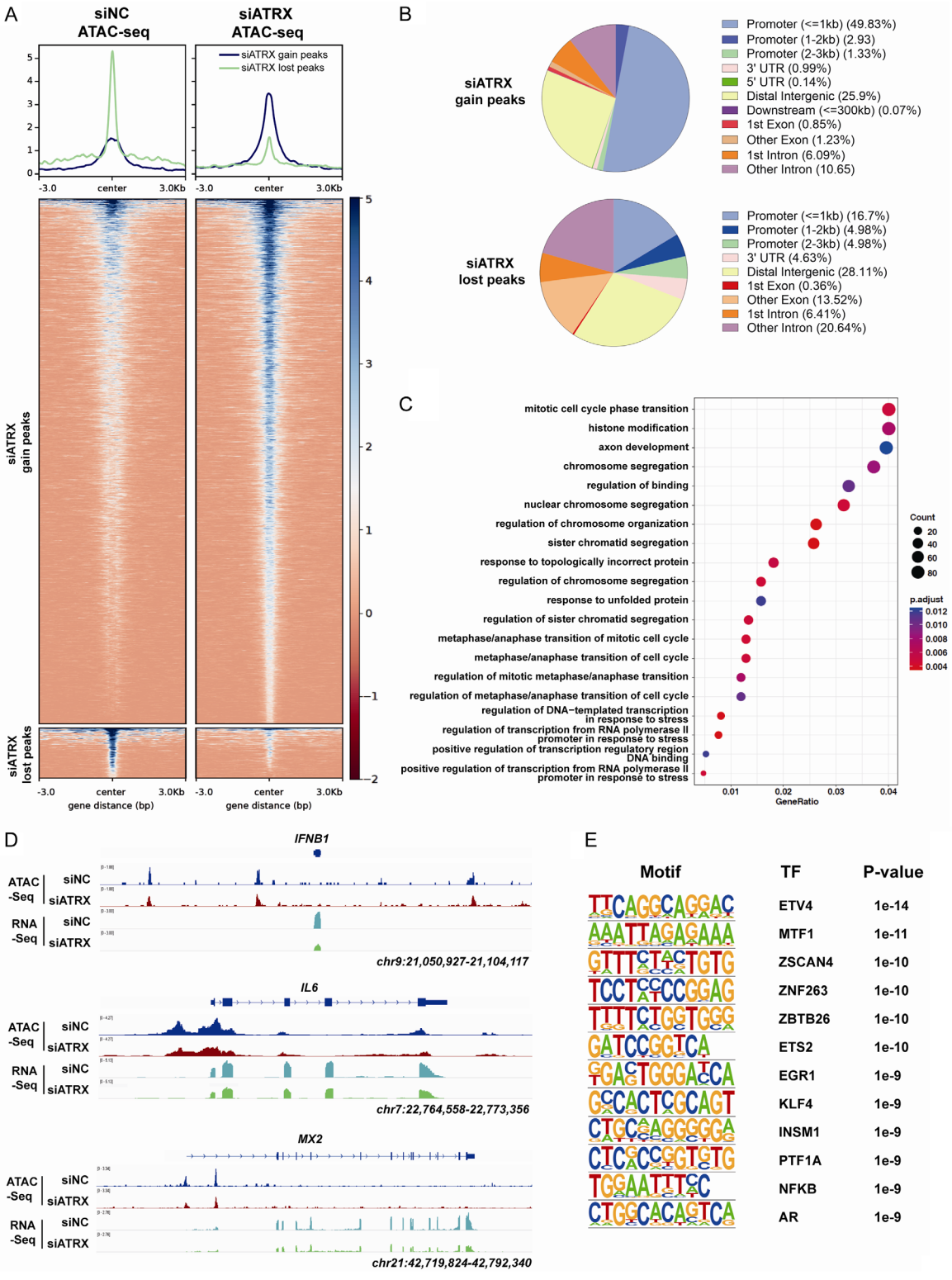

Figure 5. ATRX loss changes the chromatin accessibility of PSGs. (A) ATAC-seq analysis of the differences in chromatin accessibility in HOS cells transfected with siATRX or siNC. Cells were stimulated by poly(I:C) for 4 hr. The data are displayed in a heatmap and metaplots. (B) Annotation of the siATRX gain and loss peaks shown in (A). (C) GO enrichment analysis of the siATRX gain peaks shown in (A). (D) Knockdown of ATRX reduced chromatin accessibility and the transcription of the *IFNB1*, *IL6* and *MX2* genes. (E) The most enriched binding motifs in lost peaks of siATRX-transfected cells as determined by ATAC-seq. The data were analyzed with HOMER.

treatment strategies. In the present study, we demonstrate that ATRX loss suppresses IFN-β signaling in sarcoma cells, which may contribute to the diminished antitumor immunity in sarcoma.

Type I IFNs are key players in antitumor immunity. In the tumor microenvironment, DAMPs, such as dsDNA or RNA, are released from stressed or dead cells, activate specific PRR pathways and initiate the transcription of Type I IFNs and other cytokines [12, 27]. After secretion, Type I IFNs bind to IFNRA1/2 receptors and activate the JAK-STAT pathway, resulting in the boost of CTLs and NK cells, and the maturation of DCs [28-30]. Our results revealed that the dsDNA-induced immune response was dysfunctional in all of the sarcoma cells we evaluated, regardless of whether ATRX function had been lost, suggesting a common mechanism in sarcoma cells. This is consistent with previous reports that the major sensor of dsDNA, the cGAS/STING pathway, is abrogated in most cancers [12, 31]. However, poly(I:C) induced the expression of IFNB1 and other cytokines in ATRX-WT cells, which had been markedly suppressed after ATRX loss in sarcoma cells. Moreover, ATRX depletion globally changed the transcription of PSGs, suggesting that ATRX may play a role in other DAMP-induced type I IFN responses.

ATRX belongs to the SWI/SNF DNA-remodeling family, and its major function involves in heterochromatin formation at repetitive DNA regions, including telomeres, pericentric repeats, rDNA repeats, and endogenous retroviral elements (ERVs) [32-36]. Together with the histone chaperone DAXX, ATRX facilitates the deposition of histone variant H3.3 at these regions, resulting in a unique form of heterochromatin characterized by both histone H3K9me3 and H3.3 [15, 37]. Dysregulation of ATRX function drives DNA replication and repair stress, thereby causing genome instability, which might change gene transcription globally. Our results revealed that depletion of ATRX decreased the chromatin accessibility of a subset of PSGs, and this mechanism differs from the usual function of ATRX as a heterochromatin organizer. The underlying mechanisms should be further investigated.

Notably, ATRX has also been reported to regulate the expression of certain types of genes in different contexts. For instance, ATRX promoted the incorporation of histone H3.3 at specific transcribed genes, mainly in ancestral pseudoautosomal regions, and facilitated transcriptional elongation through G-rich sequences [38]. More recently, Han et al. reported that ATRX interacted with EZH2 and downregulated the expression of Fas-associated death domain (FADD) by attenuating H3K27me3 enrichment at the FADD promoter region [39]. Recently, Stilp et al. reported that after virus infection, ATRX interacted with the transcription factor interferon regulatory factor 3 (IRF3) and increased chromatin accessibility, thereby promoting type I interferon and interferon-stimulated gene (ISG) expression [40]. Further study is needed to determine whether these mechanisms are evident in sarcoma cells.

Previous studies have exposed multiple functions of ATRX mutants in sarcoma progression, including the activation of the ALT pathway, promotion of NF-κB and integrin signaling, and regulation of cGAS/STING signaling [18-20]. Our study provides important complementary information by showing that ATRX loss modulates the immune microenvironment by inhibiting INF-β signaling. More interestingly, ATRX depletion led to the upregulation of the genes associated with metal ion homeostasis and response after poly(I:C) stimulation, and determining whether these outcomes are evident in antitumor immunity is a worthy line of inquiry.

In conclusion, this study demonstrates that the *ATRX* mutations negatively correlated with overall survival as well as the type I IFN response in sarcoma patients. Loss of ATRX function suppressed the type I IFN response in sarcoma cells, indicating that the restoration of innate immunity is critical for the treatment of ATRX-mutant sarcoma.

Acknowledgements

We appreciate the technical support of the Center for Scientific Research in the School of Life Sciences, Anhui Medical University. This study was supported by grants from the National Natural Science Foundation of China Projects (8207112538) and the Talent Start-up Program of Anhui Medical University.

Disclosure of conflict of interest

None.

Address correspondence to: Dr. Mafei Xu, Department of Cell Biology, School of Life Sciences, Anhui Medical University, Hefei 230032, Anhui, China. E-mail: xumafei@ahmu.edu.cn

References

[1] Boddu S, Walko CM, Bienasz S, Bui MM, Henderson-Jackson E, Naghavi AO, Mullinax JE, Joyce DM, Binitie O, Letson GD, Gonzalez RJ, Reed DR, Druta M and Brohl AS. Clinical utility of genomic profiling in the treatment of advanced sarcomas: a single-center experience. JCO Precis Oncol 2018; 2: 1-8.

[2] Zhao J, Dean DC, Hornicek FJ, Yu X and Duan Z. Emerging next-generation sequencing-based discoveries for targeted osteosarcoma therapy. Cancer Lett 2020; 474: 158-167.

[3] Anderson PM. Immune therapy for sarcomas. Adv Exp Med Biol 2017; 995: 127-140.

[4] Zhu MMT, Shenasa E and Nielsen TO. Sarcomas: immune biomarker expression and checkpoint inhibitor trials. Cancer Treat Rev 2020; 91: 102115.

[5] Szeto GL and Finley SD. Integrative approaches to cancer immunotherapy. Trends Cancer 2019; 5: 400-410.

[6] Lee AY and Brady MS. Neoadjuvant immunotherapy for melanoma. J Surg Oncol 2021; 123: 782-788.

[7] Denault MH and Melosky B. Immunotherapy in the first-line setting in wild-type NSCLC. Curr Oncol 2021; 28: 4457-4470.

[8] Butt SU and Malik L. Role of immunotherapy in bladder cancer: past, present and future. Cancer Chemother Pharmacol 2018; 81: 629-645.

[9] Ayodele O and Razak ARA. Immunotherapy in soft-tissue sarcoma. Curr Oncol 2020; 27 Suppl 1: 17-23.

[10] Klemen ND, Kelly CM and Bartlett EK. The emerging role of immunotherapy for the treatment of sarcoma. J Surg Oncol 2021; 123: 730-738.

[11] Woo SR, Corrales L and Gajewski TF. Innate immune recognition of cancer. Annu Rev Immunol 2015; 33: 445-474.

[12] Borden EC. Interferons alpha and beta in cancer: therapeutic opportunities from new insights. Nat Rev Drug Discov 2019; 18: 219-234.

[13] Ablasser A and Hur S. Regulation of cGAS- and RLR-mediated immunity to nucleic acids. Nat Immunol 2020; 21: 17-29.

[14] Piras R, Ko EY, Barrett C, De Simone M, Lin X, Broz MT, Tessaro FHG, Castillo-Martin M, Cordon-Cardo C, Goodridge HS, Di Vizio D, Batish M, Lawrenson K, Chen YG, Chan KS and Guarnerio J. circCsnk1g3- and circAnkib1-regulated interferon responses in sarcoma promote tumorigenesis by shaping the immune microenvironment. Nat Commun 2022; 13: 7243.

[15] Valenzuela M, Amato R, Sgura A, Antoccia A and Berardinelli F. The multiple facets of ATRX protein. Cancers (Basel) 2021; 13: 2211.

[16] Hoang SM and O'Sullivan RJ. Alternative lengthening of telomeres: building bridges to connect chromosome ends. Trends Cancer 2020; 6: 247-260.

[17] Hoadley KA, Yau C, Hinoue T, Wolf DM, Lazar AJ, Drill E, Shen R, Taylor AM, Cherniack AD, Thorsson V, Akbani R, Bowlby R, Wong CK, Wiznerowicz M, Sanchez-Vega F, Robertson AG, Schneider BG, Lawrence MS, Noushmehr H, Malta TM; Cancer Genome Atlas Network; Stuart JM, Benz CC and Laird PW. Cell-of-origin patterns dominate the molecular classification of 10,000 tumors from 33 types of cancer. Cell 2018; 173: 291-304, e296.

[18] Ren X, Tu C, Tang Z, Ma R and Li Z. Alternative lengthening of telomeres phenotype and loss of ATRX expression in sarcomas. Oncol Lett 2018; 15: 7489-7496.

[19] Bartholf DeWitt S, Hoskinson Plumlee S, Brighton HE, Sivaraj D, Martz EJ, Zand M, Kumar V, Sheth MU, Floyd W, Spruance JV, Hawkey N, Varghese S, Ruan J, Kirsch DG, Somarelli JA, Alman B and Eward WC. Loss of ATRX promotes aggressive features of osteosarcoma with increased NF-kappaB signaling and integrin binding. JCI Insight 2022; 7: e151583.

[20] Floyd W, Pierpoint M, Su C, Patel R, Luo L, Deland K, Wisdom AJ, Zhu D, Ma Y, DeWitt SB, Williams NT, Lazarides AL, Somarelli JA, Corcoran DL, Eward WC, Cardona DM and Kirsch DG. Atrx deletion impairs CGAS/STING signaling and increases sarcoma response to radiation and oncolytic herpesvirus. J Clin Invest 2023; 133: e149310.

[21] Chen YA, Shen YL, Hsia HY, Tiang YP, Sung TL and Chen LY. Extrachromosomal telomere repeat DNA is linked to ALT development via cGAS-STING DNA sensing pathway. Nat Struct Mol Biol 2017; 24: 1124-1131.

[22] Chen T, Chen X, Zhang S, Zhu J, Tang B, Wang A, Dong L, Zhang Z, Yu C, Sun Y, Chi L, Chen H, Zhai S, Sun Y, Lan L, Zhang X, Xiao J, Bao Y, Wang Y, Zhang Z and Zhao W. The genome sequence archive family: toward explosive data growth and diverse data types. Genomics Proteomics Bioinformatics 2021; 19: 578-583.

[23] CNCB-NGDC Members and Partners. Database Resources of the national genomics data center, China National center for bioinformation in 2022. Nucleic Acids Res 2022; 50: D27-D38.

[24] Iurescia S, Fioretti D and Rinaldi M. The innate immune signalling pathways: turning RIG-I sensor activation against cancer. Cancers (Basel) 2020; 12: 3158.
[25] Luo WW, Lian H, Zhong B, Shu HB and Li S. Kruppel-like factor 4 negatively regulates cellular antiviral immune response. Cell Mol Immunol 2016; 13: 65-72.
[26] Yum S, Li M, Fang Y and Chen ZJ. TBK1 recruitment to STING activates both IRF3 and NF-κB that mediate immune defense against tumors and viral infections. Proc Natl Acad Sci U S A 2021; 118: e2100225118.
[27] Zitvogel L, Galluzzi L, Kepp O, Smyth MJ and Kroemer G. Type I interferons in anticancer immunity. Nat Rev Immunol 2015; 15: 405-414.
[28] Xu HC, Grusdat M, Pandyra AA, Polz R, Huang J, Sharma P, Deenen R, Kohrer K, Rahbar R, Diefenbach A, Gibbert K, Lohning M, Hocker L, Waibler Z, Haussinger D, Mak TW, Ohashi PS, Lang KS and Lang PA. Type I interferon protects antiviral CD8+ T cells from NK cell cytotoxicity. Immunity 2014; 40: 949-960.
[29] Papewalis C, Jacobs B, Wuttke M, Ullrich E, Baehring T, Fenk R, Willenberg HS, Schinner S, Cohnen M, Seissler J, Zacharowski K, Scherbaum WA and Schott M. IFN-alpha skews monocytes into CD56+-expressing dendritic cells with potent functional activities in vitro and in vivo. J Immunol 2008; 180: 1462-1470.
[30] Crouse J, Bedenikovic G, Wiesel M, Ibberson M, Xenarios I, Von Laer D, Kalinke U, Vivier E, Jonjic S and Oxenius A. Type I interferons protect T cells against NK cell attack mediated by the activating receptor NCR1. Immunity 2014; 40: 961-973.
[31] An X, Zhu Y, Zheng T, Wang G, Zhang M, Li J, Ji H, Li S, Yang S, Xu D, Li Z, Wang T, He Y, Zhang L, Yang W, Zhao R, Hao D and Li X. An analysis of the expression and association with immune cell infiltration of the cGAS/STING pathway in pan-cancer. Mol Ther Nucleic Acids 2019; 14: 80-89.
[32] Law MJ, Lower KM, Voon HP, Hughes JR, Garrick D, Viprakasit V, Mitson M, De Gobbi M, Marra M, Morris A, Abbott A, Wilder SP, Taylor S, Santos GM, Cross J, Ayyub H, Jones S, Ragoussis J, Rhodes D, Dunham I, Higgs DR and Gibbons RJ. ATR-X syndrome protein targets tandem repeats and influences allele-specific expression in a size-dependent manner. Cell 2010; 143: 367-378.
[33] Sadic D, Schmidt K, Groh S, Kondofersky I, Ellwart J, Fuchs C, Theis FJ and Schotta G. Atrx promotes heterochromatin formation at retrotransposons. EMBO Rep 2015; 16: 836-850.
[34] He Q, Kim H, Huang R, Lu W, Tang M, Shi F, Yang D, Zhang X, Huang J, Liu D and Songyang Z. The Daxx/Atrx complex protects tandem repetitive elements during DNA hypomethylation by promoting H3K9 trimethylation. Cell Stem Cell 2015; 17: 273-286.
[35] Voon HP, Hughes JR, Rode C, De La Rosa-Velazquez IA, Jenuwein T, Feil R, Higgs DR and Gibbons RJ. ATRX plays a key role in maintaining silencing at interstitial heterochromatic loci and imprinted genes. Cell Rep 2015; 11: 405-418.
[36] Udugama M, Sanij E, Voon HPJ, Son J, Hii L, Henson JD, Chan FL, Chang FTM, Liu Y, Pearson RB, Kalitsis P, Mann JR, Collas P, Hannan RD and Wong LH. Ribosomal DNA copy loss and repeat instability in ATRX-mutated cancers. Proc Natl Acad Sci U S A 2018; 115: 4737-4742.
[37] Voon HP and Wong LH. New players in heterochromatin silencing: histone variant H3.3 and the ATRX/DAXX chaperone. Nucleic Acids Res 2016; 44: 1496-1501.
[38] Levy MA, Kernohan KD, Jiang Y and Berube NG. ATRX promotes gene expression by facilitating transcriptional elongation through guanine-rich coding regions. Hum Mol Genet 2015; 24: 1824-1835.
[39] Han B, Meng X, Wu P, Li Z, Li S, Zhang Y, Zha C, Ye Q, Jiang C, Cai J and Jiang T. ATRX/EZH2 complex epigenetically regulates FADD/PARP1 axis, contributing to TMZ resistance in glioma. Theranostics 2020; 10: 3351-3365.
[40] Stilp AC, Scherer M, Konig P, Furstberger A, Kestler HA and Stamminger T. The chromatin remodeling protein ATRX positively regulates IRF3-dependent type I interferon production and interferon-induced gene expression. PLoS Pathog 2022; 18: e1010748.